Hydrogen atom transfer by a high-valent nickel-chloride complex

Prasenjit Mondal,[a] Paolo Pirovano,[a] Ankita Das,[a] Erik R. Farquhar,[b] Aidan R. McDonald*[a]

[a]School of Chemistry and CRANN/AMBER Nanoscience Institute, Trinity College Dublin, The University of Dublin, College Green, Dublin 2, Ireland; [b]Case Western Reserve University Center for Synchrotron Biosciences, National Synchrotron Light Source II, Brookhaven National Laboratory II, Upton, NY 11973, USA

Oxo-metal-halide moieties have often been implicated as C–H bond activating oxidants with the terminal oxo-metal entity identified as the electrophilic oxidant. The electrophilic reactivity of metal-halide species has not been investigated. We have prepared a high-valent nickel-halide complex [Ni^{III}(Cl)(L)] (**2**, L = *N,N'*-(2,6-dimethylphenyl)-2,6-pyridinedicarboxamide) by one-electron oxidation of the [Ni^{II}(Cl)(L)]$^-$ precursor. **2** was characterized using electronic absorption, electron paramagnetic resonance, and X-ray absorption spectroscopies, and mass spectrometry. **2** reacted readily with substrates containing either phenolic O–H or hydrocarbon C–H bonds. Thorough kinetic analysis of these reactions was performed. Analysis of the Hammett, Evans-Polanyi, and Marcus relationships between the determined rate constants and substrate pKa, X-H bond dissociation energy, and oxidation potential, respectively, was performed. Through this analysis we found that **2** reacted by a hydrogen atom transfer (HAT) mechanism. Our findings shine light on enzymatic high-valent oxo-metal-halide oxidants and open new avenues for oxidative halogenation catalyst design.

The selective functionalization of inert C–H bonds to a more versatile functional group has far reaching practical applications in many chemical industries.[1-10] Nature has evolved a variety of remarkably efficient metalloenzymes that functionalise inert hydrocarbons through oxidative hydroxylation, desaturation, C–X bond formation (X = O, N, S), and halogenation.[4, 7-10] To facilitate these transformations, hydrogen atom transfer (HAT) activation of the inert C–H bond is postulated to occur via a high-valent metal-based oxidant (often a metal-oxo (M=O) moiety).[4, 7-10] For such transformations catalysed by man-made catalysts, a M=O oxidant is also most often implicated.[11-17] More recent efforts have focused on the capability of metal–OX (OX = OH, OR, O_2C-R, ONO_2) and metal-imido entities in oxidative C–H bond activation,[18-28] demonstrating that a terminal M=O is not a prerequisite for hydrocarbon oxidation.

The α-ketoglutarate dependent non-heme iron halogenases (such as CytC3 and SyrB2) constitute a class of important enzymes that perform the biological *halogenation* of un-activated C–H bonds.[29-32] A non-heme halo-Fe^{IV}=O moiety is postulated to perform the initial HAT from a substrate to give a halo-Fe^{III}–OH species and a carbon-centered radical. Rebound of the halide ligand with the carbon-centered radical is proposed to result in the halogenated product.[32-34] Biomimetic halo-Fe^{IV}=O model compounds have been prepared and displayed the ability to perform oxidative halogenation of hydrocarbons in some cases.[35-40] As in the enzymatic systems, the Fe^{IV}=O unit was postulated to perform HAT followed by radical rebound with the metal-bound halide. Groves and co-workers have demonstrated remarkably efficient oxidative hydrocarbon fluorination using manganese-porphyrin catalysts.[41-42] The proposed oxidant was an F–Mn^{V}=O species that performed HAT, with rebound of the fluoride ligand with the carbon-centred radical yielding the fluorinated product. Groves has similarly demonstrated oxidative chlorination of hydrocarbons using manganese-porphyrin catalysts in conjunction with hypochlorous acid.[42] In that case, however, after initial HAT by Mn^{V}=O, a ClO-Mn^{IV} species was proposed to react with the resulting carbon-centred radical to form the C–Cl bond. Recently Costas and Browne demonstrated the chlorination of alkanes mediated by a nickel catalyst and NaOCl,[43] where a chlorine radical was postulated to bring about hydrocarbon chlorination. Overall, metal-mediated oxidative halogenation is well-established, however little insight into the HAT oxidising entity has been obtained.

Interestingly, in all of these biological, biomimetic, and catalysis studies, the HAT reactivity of the metal-bound halide in C–H activation was not considered. To the best of our knowledge, no examples of high-valent metal-halide complexes performing HAT have been reported. This is not surprising given the high electronegativity of the halogens, seemingly excluding metal-halides from performing electrophilic HAT reactions. However, we believe such species have great potential as HAT oxidants, as they could potentially eliminate oxygenated products (hydroxylation, epoxidation) from the hydrocarbon oxidation process (thus yielding solely halogenated products). Furthermore, through halide selection, simple tuning of the potency of the high-valent oxidant would be achieva-

ble. Herein, we describe the preparation and characterization of a Ni^{III}–Cl complex (**2**) that is capable of performing HAT oxidation of phenolic O–H and hydrocarbon C–H bonds.

Scheme 1. Preparation of **1** by chloride ligand exchange (Et = C_2H_5) and **2** by oxidation with $(NH_4)_2[Ce^{IV}(NO_3)_6]$ (CAN, -40 °C) *or* tris(4-bromophenyl)ammoniumyl hexachloroantimonate (magic blue, -80 °C).

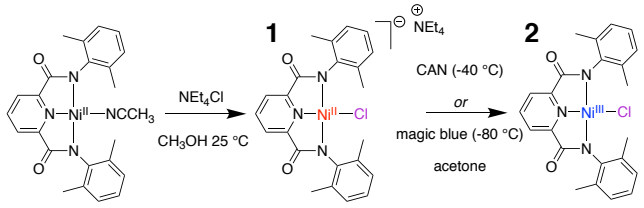

Results and discussion: $Et_4N[Ni^{II}(Cl)(L)]$ (**1**, Scheme 1, L = *N,N'*-(2,6-dimethylphenyl)-2,6-pyridinedicarboxamide, Et = ethyl), previously prepared by Holm and co-workers,[44] was synthesized using an alternative method by simple chloride ligand exchange with the previously prepared $[Ni^{II}(NCCH_3)(L)]$ (see supporting information for details).[25] **1** was obtained in 85% yield and was characterized by nuclear magnetic resonance (NMR), Fourier transform infra-red (FT-IR), and electrospray ionization mass spectrometry (ESI-MS, Figures S1-S4).

1 (0.3 mM, acetone) was reacted with $(NH_4)_2[Ce^{IV}(NO_3)_6]$ (CAN, 2 equiv., Scheme 1) in the presence of Et_4NCl (1 equiv.) at −40 °C, resulting in an immediate reaction (complete in 30 s) as evidenced by a colour change from pale orange to blue/green. Electronic absorption spectroscopy showed the appearance of a broad and intense feature in the visible region (λ_{max} = 600 nm, Figure 1) that reached a maximum after 30 s, which we assigned to a new species, **2**. In the absence of excess Et_4NCl a lower yield of **2** was obtained. **2** could also be prepared using the one-electron oxidant tris(4-bromophenyl)ammoniumyl hexachloroantimonate (magic blue). The addition of 1 equivalent of magic blue to a 0.3 mM solution of **1** (acetone, −80 °C) caused the immediate formation of the band at λ_{max} = 600 nm (Figure S6). The observation of the same product by the one-electron oxidation of **1**, would suggest that **2** was $[Ni^{III}(Cl)(L)]$. **2** displayed electronic absorption features similar to those reported for analogous Ni^{III} complexes supported by L ($[Ni^{III}(OX)(L)]$, OX = OCO_2H, O_2CCH_3, ONO_2),[25, 45] and other high valent Ni complexes,[23, 26-27, 46-49] leading us to conclude a change in the metal oxidation state, and that **2** was likely $[Ni^{III}(Cl)(L)]$.

Electron paramagnetic resonance (EPR) spectroscopy analysis of **2** showed a metal based rhombic signal (g_x = 2.32, g_y = 2.23, g_z = 2.00, Figure 1) with hyperfine splitting (g_z quartet), due to the Cl atom (I = 3/2, Figure 1)[50-51] lying in close proximity to the unpaired spin density. The average g-value (2.18) alongside the rhombic signal ($g_x > g_y >> g_z$) was consistent with the unpaired spin being localized on a low-spin d^7 Ni^{III} ion in a square planar or tetragonally distorted octahedral coordination environment.[51-58] Furthermore, the EPR spectrum compared favourably to those obtained for analogous $[Ni^{III}(OX)(L)]$ complexes.[25, 45] The yield of Ni^{III} was calculated to be 80% ± 20% by double integration of the signal obtained for **2** and comparison against the radical standard (2,2,6,6-tetramethylpiperidin-1-yl)oxyl (TEMPO). EPR spectroscopy also confirmed the presence of the same species in the preparation of **2** with magic blue (Figure S7). The obtained spectrum with Cl-hyperfine interactions supported the assignment of **2** as $[Ni^{III}(Cl)(L)]$.

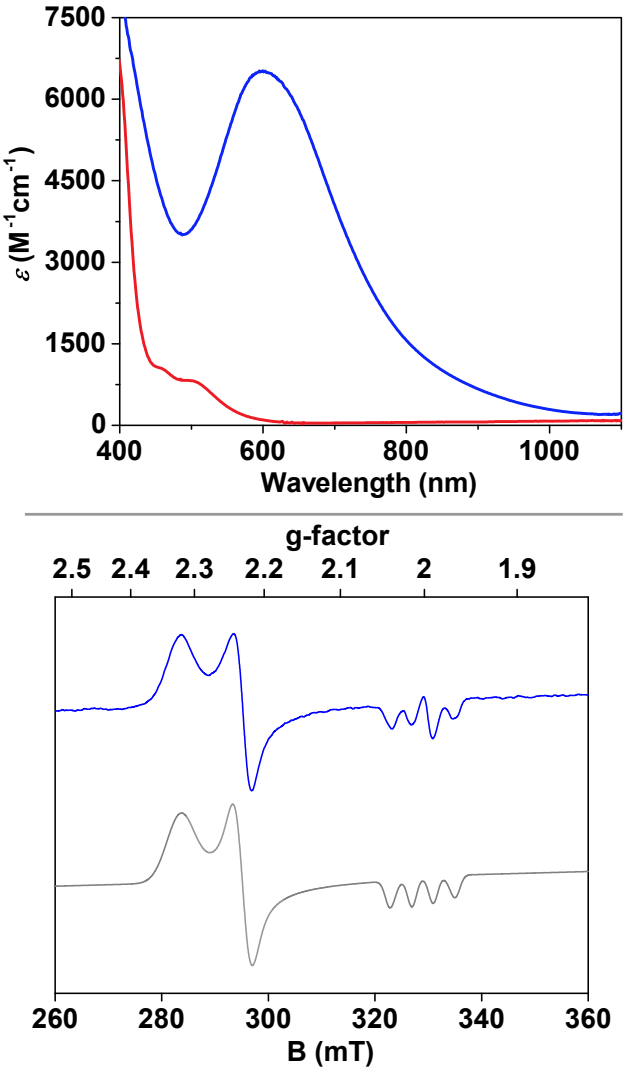

Figure 1. Top: Electronic absorption spectrum of **1** (red trace, 0.3 mM acetone solution, −40 °C) and of the oxidation product **2** (blue trace) obtained after the addition of CAN (2 equiv.). **Bottom:** X-band EPR spectrum of **2** in a frozen acetone solution (blue trace) measured at 77 K, 2 mW microwave power, with 0.7 mT modulation amplitude, and the simulated spectrum of **2** (grey trace, see supporting information for simulation details).

The elemental formula of **2** was confirmed using ESI-MS. A peak at m/z = 465 corresponding to $[\mathbf{2} + H]^+$ with the expected isotopic pattern was observed (Figure S8). It is important to note that solutions of **2** in ESI-MS positive mode always displayed this peak, however, solutions of **1** in ESI-MS positive mode did not. The Ni^{II} precursor **1**

could only be detected in the ESI-MS negative mode (as the $[Ni^{II}(Cl)(L)]^-$ fragment), consistent with previous observations.[23, 25]

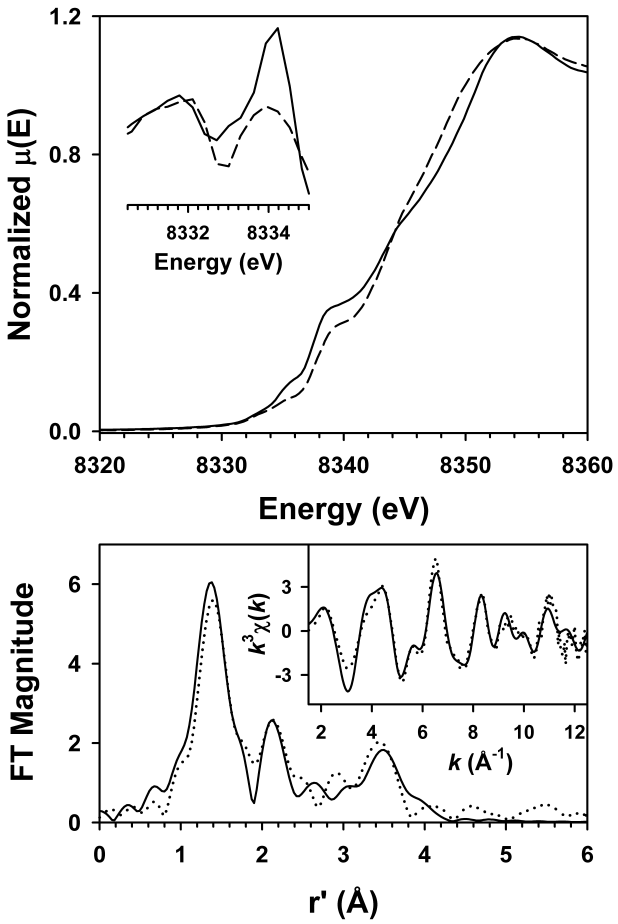

Figure 2. Top: normalised XANES spectra of **1** (solid line) and **2** (dashed line). The inset depicts the second derivative of both spectra in the pre-edge region. **Bottom**: best fit to k^3-weighted EXAFS data of **2**. Experimental data is shown as a dotted line, while the best fit is shown as a solid line.

2 was not stable enough to allow growth of crystals suitable for X-ray crystallography, we therefore performed Ni K-edge X-ray absorption spectroscopy (XAS) on a frozen solution of **2** (Figure 2). The Ni K-edge energy (8345 eV) for **2** was similar to those previously reported for Ni^{III} complexes,[59-61] and including values obtained for several $[Ni^{III}(OX)(L)]$ complexes.[25, 45] A comparison of the Ni K-edge X-ray absorption near-edge spectra (XANES) of **1** and **2** demonstrated almost no shift in the Ni K-edge. This was also observed for $[Ni^{III}(OX)(L)]$ complexes,[25, 45] and has been seen previously for other $Ni^{II/III}$ couples.[59, 62-63] Nonetheless, the shape and profile of the XANES spectra are markedly different confirming a change in the properties of **1** and **2**. We ascribe the change in the profile to contributions to the edge from 1s-to-4p + shakedown absorption features that distort the edge shape (~ 8340 eV). The weak 1s-to-3d pre-edge transitions showed a modest 0.5 eV blue shift (Figure 2) upon conversion of **1** to **2**, providing evidence for a modified ligand field, consistent with an increase in Ni oxidation state.

Extended X-ray absorption fine structure (EXAFS) analysis of **2** showed a best fit with a first coordination sphere with 3 O/N scatterers at 1.88 Å, and critically, a Cl scatterer at 2.17 Å (Figure 2, Table S1). Fitting the EXAFS data with an O/N-only first coordination sphere did not provide reliable fits of the data, with inclusion of a Cl scatterer producing a dramatic improvement in fit quality. The fit is completed with a set of single and multiple scattering paths arising from atoms of the ligand framework. The Ni^{III}–Cl bond length obtained for **2** was similar to the X-ray crystallographically determined Ni^{II}–Cl bond distance (2.174 Å) in **1**.[44] Likewise the mean Ni–N bond lengths are similar to those obtained for **1** (1.912 Å (x2) and 1.796 Å) indicating little-to-no change in the first coordination sphere upon conversion of **1** to **2**. In $[Ni^{II/III}(OX)(L)]^{o/-}$, a change in Ni oxidation state had similarly negligible influence on the metal-ligand bond lengths in the first coordination sphere in this family of complexes, which was further supported by DFT calculations.[25, 45] Importantly, the identification of a larger (Cl) scatterer in the first coordination sphere confirmed the presence of the Cl atom in **2**, alongside the ESI-MS and EPR analyses.

Reactivity Studies: A survey of the stability and oxidative reactivity of **2** in phenolic O–H and hydrocarbon C–H bond activation reactions was performed. The half-life ($t_{1/2}$) determined for **2** was approximately 6 h at -40 °C. Kinetic analysis of the reaction between **2** and substrates was followed by electronic absorption spectroscopy by monitoring the decrease in the absorbance at λ_{max} = 600 nm upon addition of substrates to **2** (Figure 3). In all cases the reactions obeyed *pseudo*-first-order kinetics. *Pseudo*-first order rate constants (k_{obs}) were found to be linearly dependent on the substrate concentration, allowing for determination of second-order rate constants (k_2) by measuring the slope of the resulting linear plot (Figure 3).

Oxidation of Phenols. Phenols have been employed as mechanistic probes for the reactivity of **2**. At -40 °C, 2,6-di-*tert*-butylphenol (2,6-DTBP, 65 equiv. dissolved in acetone) was added to **2** (0.3 mM, acetone) resulting in an immediate reaction that was complete within 150 s (Figure 3). A k_2 value of 0.176 $M^{-1}s^{-1}$ for 2,6-DTBP was determined (Figure S9). Product analysis of the reaction mixture revealed the formation of a radical coupling product 3,3′,5,5′-tetra-*tert*-butyl-[1,1′-bis(cyclohexane)]-2,2′,5,5′-tetraene-4,4′-dione, as detected by ESI-MS (Scheme S1). The product likely derived from coupling of two phenoxyl radicals. The same reaction when performed with 2,4-di-*tert*-butylphenol (2,4-DTBP) resulted in a rate constant value of k_2 = 4.77 $M^{-1}s^{-1}$ (Figure S10). Again, a radical coupling product (3,3′,5,5′-tetra-*tert*-butyl-[1,1′-bis(cyclohexane)]-4,4′,6,6′-tetraene-2,2′-dione, Scheme S1) was identified, again presumably formed from the reaction of two phenoxyl radicals. Both substrates have similar O–H bond dissociation energies (~82 kcal mol^{-1}),[64-67] although 2,4-DTBP is expected to react considerably faster in HAT because of the decreased steric bulk around the O–H group.[25, 68-71] Differing reaction rates between these two sterically different substrates by the same oxidant has

previously been considered to imply a HAT mechanism.[68] The ~30-fold difference in relative reactivity for **2** is consistent with a HAT mechanism, but is slightly small compared to previous reports (>50 fold).[25, 68-71] Based on the products identified, and the difference in reactivity of these substrates, the mechanism of phenol oxidation thus can be ascribed to HAT.

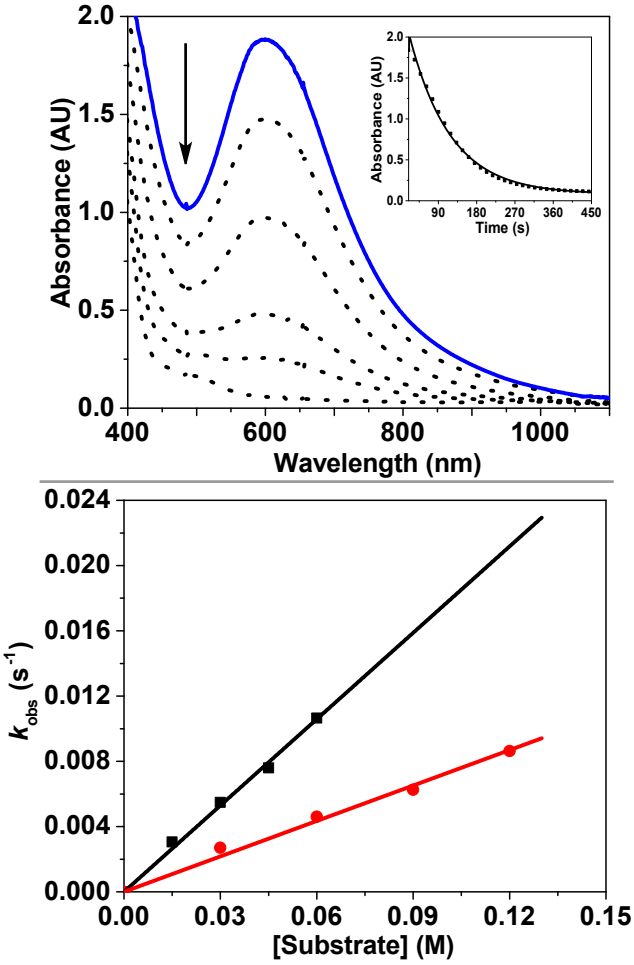

Figure 3. Top: changes in the electronic absorption spectrum during the decay of **2** (blue trace) in the presence of 65 equivalents of 2,6-DTPB, at –40 °C. Inset: time trace of the absorbance at λ_{max} = 600 nm. **Bottom**: plots of k_{obs} versus [*H*/*D*-2,6-DTBP] determined for the reactions between **2** and [*H*]2,6-DTBP (black) and [*D*]2,6-DTBP (red), at –40 °C in acetone.

In order to probe the oxidation mechanism further, the reaction of **2** with deuterated 2,6-DTBP was explored. [*D*]-2,6-DTBP yielded a k_2 value of 0.072 $M^{-1}s^{-1}$ (Figure 3, 0.176 $M^{-1}s^{-1}$ for [*H*]-2,6-DTBP). The obtained kinetic isotope effect (KIE) value of 2.4 indicated that O–H bond cleavage was involved in the rate-determining step, and was consistent with a HAT mechanism. The KIE was rather small compared to M=O oxidants which generally display KIE values >7 for HAT.[72-75] Importantly, however, the obtained KIE value closely matched KIE values (range 2-3) determined for other high-valent Ni oxidants that were shown to perform HAT.[24-28]

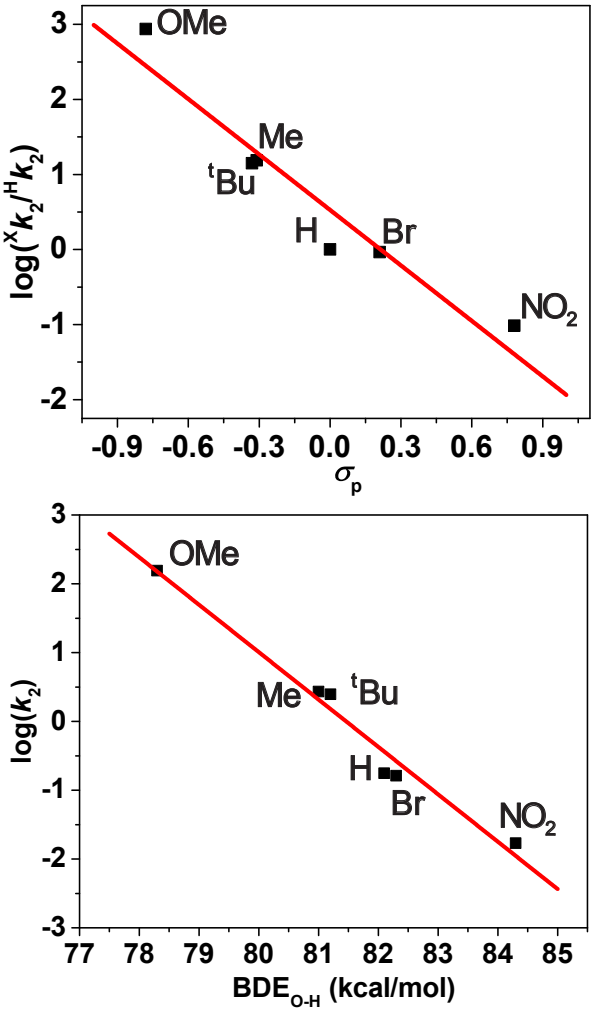

Figure 4. Top: Hammett correlation plot for the reaction of **2** with *p*-X-2,6-DTBP substrates; **Bottom**: plot of $\log(k_2)$ versus BDE_{O-H} for *p*-X-2,6-DTBP.

To gain a better understanding of the mechanism of phenol oxidation by **2**, a series of *para*-substituted 2,6-di-*tert*-butylphenol substrates (*p*-X-2,6-DTBP, X = OCH_3, $C(CH_3)_3$, CH_3, Br, NO_2) were reacted with **2** (Figures S11-S15). All substrates reacted readily with **2**. GC-MS analyses indicated the formation of 2,6-di-*tert*-butyl-1,4-benzoquinone in the cases of *p*-OCH_3- and *p*-CH_3-2,6-DTBP (Scheme S1). All substrates displayed a linear dependence of k_{obs} against [*p*-X-2,6-DTBP] allowing for k_2 values for all substrates to be determined (Table S2). We have plotted the obtained k_2-values against the substrate Hammett σ_p-parameter and the substrate O–H bond dissociation free energy (BDE_{O-H}, Figure 4).

The Hammett analysis showed a decrease in the k_2 value with more electron-poor substrates (thus k_2(*p*-OCH_3-2,6-DTBP) >> k_2(*p*-NO_2-2,6-DTBP), Figure 4). A slope of ρ = –2.5 was obtained for the Hammett plot. Such a linear relationship in the Hammett plot with a negative slope indicated that concerted PCET (thus HAT) was the most likely mechanism in phenol oxidation.[68, 76-81] The plot of the log of k_2 against the phenol BDE_{O-H} also demonstrated a linear relationship (Figure 4). As extensively document-

ed by Mayer for metal-based oxidants,[82-83] this is expected for a HAT mechanism, in which BDE's govern the ΔH° of the reaction, and is thus a strong indication of a HAT rate-determining step. Deriving Gibbs energies of activation from the measured k_2 values, a $\Delta G^{\ddagger}/\Delta(BDE)$ slope of 0.69 was determined. We previously observed that $[Ni^{III}(O_2CCH_3)(L)]$ displayed a slope of 0.31 for hydrocarbon C–H HAT activation.[25] These values compare favourably with the ideal $\Delta G^{\ddagger}/\Delta G^{\circ}$ value of 0.5 for HAT predicted by Marcus theory,[84-85] and with previously reported experimental values in the range of 0.15 to 0.7 for other metal-based oxidants that perform HAT.[74, 86-92]

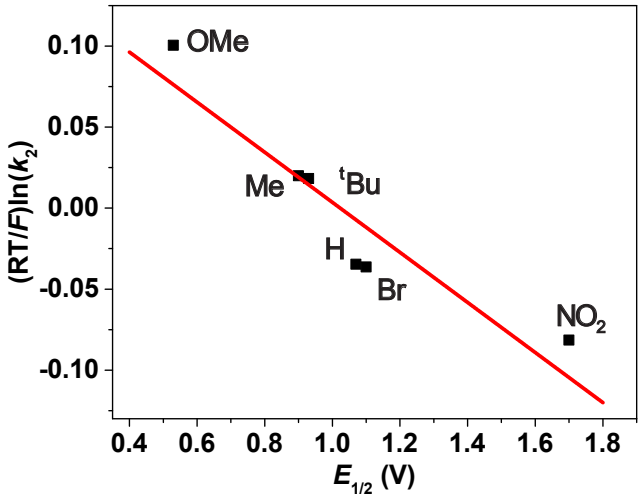

Figure 5. Plot of (RT/F)ln(k_2) against the oxidation potential (E) of *p*-X-2,6-DTBP substrates for the reactions of **2** with *p*-X-2,6-DTBP substrates in acetone.

A plot of (RT/F)ln(k_2) *versus* the oxidation potentials (E_{ox}) of the phenols (Figure 5) showed a good linear correlation with ln(k_2) decreasing with decreasing E_{ox} affording a slope of 0.15. Such plots have been employed to understand the mechanisms of proton coupled electron transfer (PCET, HAT is a member of this family) reactions. If the reaction involved slow (rate-limiting) electron transfer from phenols followed by a fast proton transfer, the slope of the Marcus plot ((RT/F)ln(k_2) versus E_{ox})[93] would be expected to be 0.5.[94] If proton transfer was rate limiting and electron transfer was in equilibrium, the slope is predicted be 1.0. For coupled non-concerted PCET mechanisms (thus non-HAT) where electron transfer and proton transfer display similar rates, a slope is predicted to lie between 0.5 and 1.0.[65, 94-96] The observed near-zero slope of 0.15 obtained for **2** (Figure 5), thus clearly rules out these PCET reaction profiles. Critically, however, for HAT (concerted PCET) a slope of close to 0.00 is predicted and has been previously observed.[65, 97-100] These combined observations confirm the reaction of the high-valent nickel-halide **2** in oxidative O–H bond activation is by a HAT mechanism.

Oxidation of Hydrocarbons. We investigated further the reactivity of **2** in hydrocarbon C–H bond activation. At 10 °C, 1,4-cyclohexadiene (CHD) reacted slowly with **2** yielding a $k_2 = 5.5 \times 10^{-4}$ $M^{-1}s^{-1}$ (Figures S16-S17). The oxidized product benzene was identified from the reaction with CHD, which is consistent with HAT initiated oxidation of the CHD. Likewise, xanthene was oxidized by **2**, with a k_2 value of 1.04×10^{-3} $M^{-1}s^{-1}$ (Figure S18) yielding xanthone. The slightly higher rate constant for xanthene oxidation is consistent with xanthene (BDE = 74 kcal mol^{-1}) containing a weaker C–H bond than CHD (BDE = 76 kcal mol^{-1}), according to the Polanyi correlation.[88, 101] These combined observations suggest that **2** (a high-valent metal-halide) will mediate the oxidation of hydrocarbon substrates, suggesting that enzymatic high-valent metal-halides may also be capable of such reactivity.

Mechanism Discussion: Our results demonstrate the capability of **2** in the activation of both O–H and C–H bonds through HAT, yielding oxygen- or carbon-based radicals, respectively. These organic radicals decay further yielding the identified oxygenated, desaturated, or coupled products. Halide incorporation (chlorinated products) was not observed for any of the hydrocarbon or phenolic oxidation products even if the oxidation was performed in the presence of excess Et_4NCl. Interestingly, however, the rate of the oxidation reaction by **2** *was* influenced by the presence of free $^{-}$Cl anion (Figure S19). The oxidation of *p*-CH_3-2,6-DTBP demonstrated a first order dependence on [$^{-}$Cl]. This would suggest that $^{-}$Cl competes with the phenolic substrate for interaction with **2** during the oxidation reaction.

An important consideration is the fate of the chloride ligand after HAT (Scheme 2). We propose that HAT results in the formation of HCl and $[Ni^{II}(L)]$. Post reaction analysis of the **2** + 2,4,6-TTBP reaction showed an electronic absorption spectrum (Figure S20) that displayed features similar to **1**, but at much lower intensity. It is worth recalling that there is a slight excess of $^{-}$Cl present in the solution (from the preparation of **2**). We surmise a small quantity of **1** forms in the reaction mixture from the interaction between $[Ni^{II}(L)]$ and this residual $^{-}$Cl. The post-reaction mixture was EPR silent. Addition of Et_4NCl to this reaction mixture gave almost quantitative reformation of **1** according to electronic absorption spectroscopy (Figure S20). This would suggest that $[Ni^{II}(L)]$ is present in the reaction mixture after **2** oxidised the phenolic substrate. Fascinatingly, addition of 4 equiv. of CAN to this solution yielded the formation of **2** *again* (Figure S21), albeit in lower yield, presumably because of the presence of a large excess of the 2,4,6-TTBP substrate. These observations confirm that the $[Ni^{II}(L)]$ core remains intact during the preparation of **2**, and after the substrate oxidation reaction mediated by **2**. Furthermore, it demonstrates that **2** can be re-generated by simple addition of a $^{-}$Cl source and CAN, meaning the system has catalytic capabilities.

We previously demonstrated that the ancillary (OX) ligand has a large effect on the relative reactivity of $[Ni^{III}(OX)(L)]$ complexes (OX = O_2CCH_3, ONO_2, OCO_2H), where $[Ni^{III}(ONO_2)(L)]$ displayed a ~20-fold greater k_2-value than the other complexes.[25, 45] These complexes were originally all prepared under different conditions than were used to prepare **2**, therefore a fair comparison to **2** of their reactivity properties was not possible.

$[Ni^{III}(ONO_2)(L)]$ can be prepared, however, under the exact same conditions as the preparation of **2** (CAN as oxidant).[25, 45] In the oxidation of *p*-CH_3-2,6-DTBP, $[Ni^{III}(ONO_2)(L)]$ displayed a k_2 value of 5.12 $M^{-1}s^{-1}$ (Figure S22), whereas **2** gave a k_2 value of 2.71 $M^{-1}s^{-1}$ (Figure S14). This demonstrates that simple tuning of the ancillary ligand can allow tuning (Cl versus ONO_2) of the HAT reactivity of the high-valent oxidant, presumably as a result of tuning the strength of the X–H bond (Ni^{II}(H–ONO_2) for $[Ni^{III}(ONO_2)(L)]$; H–Cl for **2**) in the product.

Scheme 2. Mechanism of HAT by **2** in C–H activation by HAT.

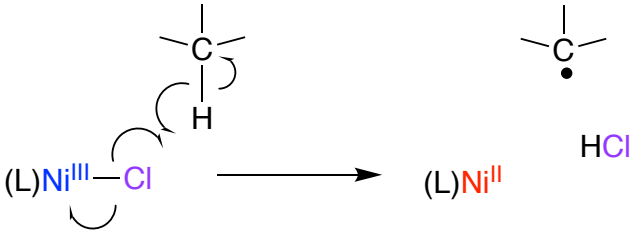

Previous reports have demonstrated the importance of the magnitude of BDE_{O-H} in M^{n-1}–O–H products formed as a result of HAT by M^n=O oxidants in defining the potency of an oxidant.[85, 102] For **2**, thus, the products of the reaction are $[Ni^{II}(L)]$ and HCl (Scheme 2). We therefore conclude that the thermodynamic driving force for the reaction of **2** with O–H or C–H bonds ($BDE_{O/C-H}$ = 76-82 kcal/mol) is the relative strength of the H–Cl bond (103 kcal mol^{-1}).[103] We postulate that this opens a unique pathway to consider hydrocarbon oxidation catalysis using high-valent metal halides, where one could simply tune the properties of the halide (F, Cl, Br, I) to enhance/tune the oxidative reactivity. Furthermore, our findings demonstrate the potential to remove the O-atom from oxidation catalysis, thus eliminating unwanted hydroxylation or epoxidation outcomes in oxidative halogenation and desaturation reactions.

Conclusions: We have presented the preparation of a Ni^{III}–Cl complex that has been characterized using electronic absorption, EPR, and XAS spectroscopies, and mass spectrometry. The Ni^{III}–Cl complex displayed the ability to oxidatively activate phenolic O–H and hydrocarbon C–H bonds, and through thorough kinetic analysis was confirmed to react by a HAT mechanism. Our findings shine light on enzymatic high-valent metal-halide oxidants and, more critically, open new avenues for oxidation catalyst design through the development of halide-only oxygen-free oxidants. Work continues in our lab to explore the mechanism of HAT by metal-halides and to probe the potential of such oxidants in oxidation catalysis.

Acknowledgements: This publication has emanated from research supported by the European Union (FP7-333948, ERC-2015-STG-678202). Research in the McDonald lab is supported in part by research grants from Science Foundation Ireland (SFI/12/RC/2278, SFI/15/RS-URF/3307). XAS experiments were conducted at SSRL beamline 2-2 (SLAC National Accelerator Laboratory, USA), with support from the DOE Office of Science (DE-AC02-76SF00515 and DE-SC0012704) and NIH (P30-EB-009998). We are grateful to COST Action CM1305 (ECOSTBio) for networking support. We are grateful to Prof. Robert Barkley for training on and use of an EPR spectrometer.

ASSOCIATED CONTENT

Supporting Information

Included in supporting information file (.pdf): physical methods; synthesis methods; reactivity protocols and results; further EPR analysis; X-ray absorption spectroscopy methods and data.

The Supporting Information is available free of charge on the ACS Publications website.

AUTHOR INFORMATION

Corresponding Author

Aidan R. McDonald, aidan.mcdonald@tcd.ie

REFERENCES

1. Sheldon, R. A.; Kochi, J. K., *Metal-Catalytzed Oxidation of Organic Compounds*. Academic: New York, 1981.
2. Arakawa, H.; Aresta, M.; Armor, J. N.; Barteau, M. A.; Beckman, E. J.; Bell, A. T.; Bercaw, J. E.; Creutz, C.; Dinjus, E.; Dixon, D. A.; Domen, K.; DuBois, D. L.; Eckert, J.; Fujita, E.; Gibson, D. H.; Goddard, W. A.; Goodman, D. W.; Keller, J.; Kubas, G. J.; Kung, H. H.; Lyons, J. E.; Manzer, L. E.; Marks, T. J.; Morokuma, K.; Nicholas, K. M.; Periana, R.; Que, L.; Rostrup-Nielson, J.; Sachtler, W. M. H.; Schmidt, L. D.; Sen, A.; Somorjai, G. A.; Stair, P. C.; Stults, B. R.; Tumas, W., *Chem. Rev.* **2001,** *101* (4), 953-996.
3. Labinger, J. A.; Bercaw, J. E., *Nature* **2002,** *417*, 507.
4. Que, L., Jr.; Tolman, W. B., *Nature* **2008,** *455*, 333-340.
5. Crabtree, R. H., *Chem. Rev.* **2010,** *110* (2), 575-575.
6. Bordeaux, M.; Galarneau, A.; Drone, J., *Angew. Chem. Int. Ed.* **2012,** *51* (43), 10712-10723.
7. Garcia-Bosch, I.; Prat, I.; Ribas, X.; Costas, M. In *Bioinspired oxidations catalyzed by nonheme iron and manganese complexes*, Wiley-VCH Verlag GmbH & Co. KGaA: 2012; pp 27-46.
8. Talsi, E. P.; Bryliakov, K. P., *Coord. Chem. Rev.* **2012,** *256* (13-14), 1418-1434.
9. Saisaha, P.; de Boer, J. W.; Browne, W. R., *Chem. Soc. Rev.* **2013,** *42* (5), 2059-2074.
10. Oloo, W. N.; Que Jr, L., 6.26 - Hydrocarbon Oxidations Catalyzed by Bio-Inspired Nonheme Iron and Copper Catalysts. In *Comprehensive Inorganic Chemistry II (Second Edition)*, Reedijk, J.; Poeppelmeier, K., Eds. Elsevier: Amsterdam, 2013; pp 763-778.
11. MacBeth, C. E.; Golombek, A. P.; Young, V. G., Jr.; Yang, C.; Kuczera, K.; Hendrich, M. P.; Borovik, A. S., *Science* **2000,** *289*, 938-941.
12. Borovik, A. S., *Chem. Soc. Rev.* **2011,** *40* (4), 1870-1874.
13. Winkler, J.; Gray, H., Electronic Structures of Oxo-Metal Ions. In *Struct Bond*, Mingos, D. M. P.; Day, P.; Dahl, J. P., Eds. Springer Berlin Heidelberg: 2012; Vol. 142, pp 17-28.
14. McDonald, A. R.; Que Jr, L., *Coord. Chem. Rev.* **2013,** *257* (2), 414-428.
15. de Visser, S. P.; Rohde, J.-U.; Lee, Y.-M.; Cho, J.; Nam, W., *Coord. Chem. Rev.* **2013,** *257* (2), 381-393.
16. Puri, M.; Que, L., Jr., *Acc. Chem. Res.* **2015,** *48* (8), 2443-2452.

17. Engelmann, X.; Monte-Perez, I.; Ray, K., *Angew. Chem. Int. Ed.* **2016,** *55* (27), 7632-7649.

18. Berry, J. F., *Comments on Inorganic Chemistry* **2009,** *30* (1-2), 28-66.

19. Pfaff, F. F.; Heims, F.; Kundu, S.; Mebs, S.; Ray, K., *Chem. Commun.* **2012,** *48*, 3730-3732.

20. Ray, K.; Heims, F.; Pfaff, F. F., *Eur. J. Inorg. Chem.* **2013,** *2013* (22-23), 3784-3807.

21. Zhang, L.; Liu, Y.; Deng, L., *J. Am. Chem. Soc.* **2014,** *136* (44), 15525-15528.

22. Zolnhofer, E. M.; Käß, M.; Khusniyarov, M. M.; Heinemann, F. W.; Maron, L.; van Gastel, M.; Bill, E.; Meyer, K., *J. Am. Chem. Soc.* **2014,** *136* (42), 15072-15078.

23. Corona, T.; Pfaff, F. F.; Acuña-Parés, F.; Draksharapu, A.; Whiteoak, C. J.; Martin-Diaconescu, V.; Lloret-Fillol, J.; Browne, W. R.; Ray, K.; Company, A., *Chem. Eur. J.* **2015,** *21* (42), 15029-15038.

24. Pirovano, P.; Farquhar, E. R.; Swart, M.; Fitzpatrick, A. J.; Morgan, G. G.; McDonald, A. R., *Chem. Eur. J.* **2015**, n/a-n/a.

25. Pirovano, P.; Farquhar, E. R.; Swart, M.; McDonald, A. R., *J. Am. Chem. Soc.* **2016,** *138* (43), 14362-14370.

26. Corona, T.; Company, A., *Chem. Eur. J.* **2016,** *22* (38), 13422-13429.

27. Corona, T.; Draksharapu, A.; Padamati, S. K.; Gamba, I.; Martin-Diaconescu, V.; Acuña-Parés, F.; Browne, W. R.; Company, A., *J. Am. Chem. Soc.* **2016,** *138* (39), 12987-12996.

28. Corona, T.; Ribas, L.; Rovira, M.; Farquhar, E. R.; Ribas, X.; Ray, K.; Company, A., *Angew. Chem. Int. Ed.* **2016,** *55* (45), 14005-14008.

29. Vaillancourt, F. H.; Yeh, E.; Vosburg, D. A.; Garneau-Tsodikova, S.; Walsh, C. T., *Chem. Rev.* **2006,** *106*, 3364-3378.

30. Galonic, D. P.; Barr, E. W.; Walsh, C. T.; Bollinger, J. M., Jr.; Krebs, C., *Nature Chem. Biol.* **2007,** *3*, 113-116.

31. Matthews, M. L.; Neumann, C. S.; Miles, L. A.; Grove, T. L.; Booker, S. J.; Krebs, C.; Walsh, C. T.; Bollinger, J. M., Jr., *Proc. Nat. Acad. Sci. USA* **2009,** *106*, 17723-17728.

32. Wong, S. D.; Srnec, M.; Matthews, M. L.; Liu, L. V.; Kwak, Y.; Park, K.; Bell Iii, C. B.; Alp, E. E.; Zhao, J.; Yoda, Y.; Kitao, S.; Seto, M.; Krebs, C.; Bollinger, J. M.; Solomon, E. I., *Nature* **2013,** *499* (7458), 320-323.

33. Krebs, C.; Galonić Fujimori, D.; Walsh, C. T.; Bollinger, J. M., Jr., *Acc. Chem. Res.* **2007,** *40*, 484-492.

34. Srnec, M.; Solomon, E. I., *J. Am. Chem. Soc.* **2017,** *139* (6), 2396-2407.

35. Rohde, J.-U.; Stubna, A.; Bominaar, E. L.; Münck, E.; Nam, W.; Que, L., Jr., *Inorg. Chem.* **2006,** *45*, 6435-6445.

36. Comba, P.; Wunderlich, S., *Chem. Eur. J.* **2010,** *16* (24), 7293-7299.

37. England, J.; Guo, Y.; Van, H. K. M.; Cranswick, M. A.; Rohde, G. T.; Bominaar, E. L.; Munck, E.; Que, L., *J. Am. Chem. Soc.* **2011,** *133*, 11880-11883.

38. Planas, O.; Clemancey, M.; Latour, J.-M.; Company, A.; Costas, M., *Chem. Commun.* **2014,** *50* (74), 10887-10890.

39. Chatterjee, S.; Paine, T. K., *Angew. Chem. Int. Ed.* **2016,** *55* (27), 7717-7722.

40. Puri, M.; Biswas, A. N.; Fan, R.; Guo, Y.; Que, L., *J. Am. Chem. Soc.* **2016,** *138* (8), 2484-2487.

41. Liu, W.; Huang, X.; Cheng, M.-J.; Nielsen, R. J.; Goddard, W. A., III; Groves, J. T., *Science* **2012,** *337* (6100), 1322-1325.

42. Liu, W.; Groves, J. T., *Acc. Chem. Res.* **2015,** *48* (6), 1727-1735.

43. Draksharapu, A.; Codolà, Z.; Gómez, L.; Lloret-Fillol, J.; Browne, W. R.; Costas, M., *Inorg. Chem.* **2015,** *54* (22), 10656-10666.

44. Huang, D.; Holm, R. H., *J. Am. Chem. Soc.* **2010,** *132* (13), 4693-4701.

45. Pirovano, P.; Farquhar, E. R.; Swart, M.; Fitzpatrick, A. J.; Morgan, G. G.; McDonald, A. R., *Chem. Eur. J.* **2015,** *21* (9), 3785-3790.

46. Kruger, H. J.; Holm, R. H., *J. Am. Chem. Soc.* **1990,** *112*, 2955-2963.

47. Corker, J. M.; Evans, J.; Levason, W.; Spicer, M. D.; Andrews, P., *Inorg. Chem.* **1991,** *30*, 331-334.

48. Patra, A. K.; Mukherjee, R., *Inorg. Chem.* **1999,** *38*, 1388-1393.

49. Chiou, T.-W.; Liaw, W.-F., *Inorg. Chem.* **2008,** *47*, 7908-7913.

50. Desideri, A.; Raynor, J. B., *J. Chem. Soc., Dalton Trans.* **1977,** (20), 2051-2054.

51. Haines, R. I.; McAuley, A., *Coord. Chem. Rev.* **1981,** *39*, 77-119.

52. Lovecchio, F. V.; Gore, E. S.; Busch, D. H., *J. Am. Chem. Soc.* **1974,** *96*, 3109-3118.

53. Jacobs, S. A.; Margerum, D. W., *Inorg. Chem.* **1984,** *23*, 1195-1201.

54. Collins, T. J.; Nichols, T. R.; Uffelman, E. S., *J. Am. Chem. Soc.* **1991,** *113* (12), 4708-9.

55. Kruger, H. J.; Peng, G.; Holm, R. H., *Inorg. Chem.* **1991,** *30*, 734-742.

56. Alonso, P. J.; Falvello, L. R.; Forniés, J.; Martín, A.; Menjón, B.; Rodríguez, G., *Chem. Commun.* **1997,** *2*, 503-504.

57. Stuart, J. N.; Goerges, A. L.; Zaleski, J. M., *Inorg. Chem.* **2000,** *39*, 5976-5984.

58. Ottenwaelder, X.; Ruiz-García, R.; Blondin, G.; Carasco, R.; Cano, J.; Lexa, D.; Journaux, Y.; Aukauloo, A., *Chem. Commun.* **2004**, 504-505.

59. Colpas, G. J.; Maroney, M. J.; Bagyinka, C.; Kumar, M.; Willis, W. S.; Suib, S. L.; Mascharak, P. K.; Baidya, N., *Inorg. Chem.* **1991,** *30*, 920-928.

60. Kundu, S.; Pfaff, F. F.; Miceli, E.; Zaharieva, I.; Herwig, C.; Yao, S.; Farquhar, E. R.; Kuhlmann, U.; Bill, E.; Hildebrandt, P.; Dau, H.; Driess, M.; Limberg, C.; Ray, K., *Angew. Chem. Int. Ed.* **2013,** *52*, 5622-5626.

61. Cho, J.; Kang, H. Y.; Liu, L. V.; Sarangi, R.; Solomon, E. I.; Nam, W., *Chem. Sci.* **2013,** *4*, 1502-1508.

62. Davidson, G.; Choudhury, S. B.; Gu, Z.; Bose, K.; Roseboom, W.; Albracht, S. P. J.; Maroney, M. J., *Biochemistry* **2000,** *39*, 7468-7479.

63. Haumann, M.; Porthun, A.; Buhrke, T.; Liebisch, P.; Meyer-Klaucke, W.; Friedrich, B.; Dau, H., *Biochemistry* **2003,** *42*, 11004-11015.

64. Wright, J. S.; Johnson, E. R.; DiLabio, G. A., *J. Am. Chem. Soc.* **2001,** *123* (6), 1173-1183.

65. Osako, T.; Ohkubo, K.; Taki, M.; Tachi, Y.; Fukuzumi, S.; Itoh, S., *J. Am. Chem. Soc.* **2003,** *125* (36), 11027-11033.

66. Grampp, G.; Landgraf, S.; Mureşanu, C., *Electrochimica Acta* **2004,** *49* (4), 537-544.

67. Jover, J.; Bosque, R.; Sales, J., *QSAR & Combinatorial Science* **2007,** *26* (3), 385-397.

68. Yiu, D. T. Y.; Lee, M. F. W.; Lam, W. W. Y.; Lau, T.-C., *Inorg. Chem.* **2003,** *42* (4), 1225-1232.

69. Lansky, D. E.; Goldberg, D. P., *Inorg. Chem.* **2006,** *45*, 5119-5125.

70. Barman, P.; Vardhaman, A. K.; Martin, B.; Wörner, S. J.; Sastri, C. V.; Comba, P., *Angew. Chem. Int. Ed.* **2015,** *54* (7), 2095-2099.

71. Kafentzi, M.-C.; Orio, M.; Reglier, M.; Yao, S.; Kuhlmann, U.; Hildebrandt, P.; Driess, M.; Simaan, A. J.; Ray, K., *Dalton Trans.* **2016,** *45* (40), 15994-16000.

72. Kaizer, J.; Klinker, E. J.; Oh, N. Y.; Rohde, J.-U.; Song, W. J.; Stubna, A.; Kim, J.; Münck, E.; Nam, W.; Que, L., Jr., *J. Am. Chem. Soc.* **2004,** *126*, 472-473.

73. Fiedler, A. T.; Que Jr, L.,*Inorg. Chem.* **2009,** *48* (23), 11038-11047.

74. Klinker, E. J.; Shaik, S.; Hirao, H.; Que, L., Jr, *Angew. Chem. Int. Ed.* **2009,** *48*, 1291-1295.

75. Yoon, J.; Wilson, S. A.; Jang, Y. K.; Seo, M. S.; Nehru, K.; Hedman, B.; Hodgson, K. O.; Bill, E.; Solomon, E. I.; Nam, W., *Angew. Chem. Int. Ed.* **2009,** *48*, 1257-1260.

76. Mahoney, L. R.; DaRooge, M. A., *J. Am. Chem. Soc.* **1970,** *92* (4), 890-899.

77. Pratt, D. A.; Dilabio, G. A.; Mulder, P.; Ingold, K. U., *Acc. Chem. Res.* **2004,** *37*, 334-340.

78. Lansky, D. E.; Goldberg, D. P., *Inorg. Chem.* **2006,** *45* (13), 5119-5125.

79. Seo, M. S.; Kim, N. H.; Cho, K.-B.; So, J. E.; Park, S. K.; Clemancey, M.; Garcia-Serres, R.; Latour, J.-M.; Shaik, S.; Nam, W., *Chem. Sci.* **2011,** *2*, 1039-1045.

80. Cho, J.; Jeon, S.; Wilson, S. A.; Liu, L. V.; Kang, E. A.; Braymer, J. J.; Lim, M. H.; Hedman, B.; Hodgson, K. O.; Valentine, J. S.; Solomon, E. I.; Nam, W., *Nature* **2011,** *478* (7370), 502-505.

81. Cho, J.; Woo, J.; Eun Han, J.; Kubo, M.; Ogura, T.; Nam, W., *Chem. Sci.* **2011,** *2* (10), 2057-2062.

82. Mayer, J. M., *Ann. Rev. Phys. Chem.* **2004,** *55*, 363-390.

83. Mayer, J. M., *Acc. Chem. Res.* **2010,** *44* (1), 36-46.

84. Roth, J. P.; Lovell, S.; Mayer, J. M., *J. Am. Chem. Soc.* **2000,** *122*, 5486-5498.

85. Mayer, J. M., *Acc. Chem. Res.* **2011,** *44*, 36-46.

86. Gardner, K. A.; Kuehnert, L. L.; Mayer, J. M., *Inorg. Chem.* **1997,** *36*, 2069-2078.

87. Goldsmith, C. R.; Jonas, R. T.; Stack, T. D. P., *J. Am. Chem. Soc.* **2002,** *124*, 83-96.

88. Bryant, J. R.; Mayer, J. M., *J. Am. Chem. Soc.* **2003,** *125*, 10351-10361.

89. Yin, G.; Danby, A. M.; Kitko, D.; Carter, J. D.; Scheper, W. M.; Busch, D. H., *J. Am. Chem. Soc.* **2008,** *130*, 16245-16253.

90. Wang, D.; Zhang, M.; Buhlmann, P.; Que, L., Jr., *J. Am. Chem. Soc.* **2010,** *132*, in press.

91. Dhar, D.; Tolman, W. B., *J. Am. Chem. Soc.* **2015,** *137* (3), 1322-1329.

92. Mandal, D.; Shaik, S., *J. Am. Chem. Soc.* **2016,** *138* (7), 2094-2097.

93. Marcus, R. A.; Sutin, N., *Biochimica et Biophysica Acta (BBA) - Reviews on Bioenergetics* **1985,** *811* (3), 265-322.

94. Ram, M. S.; Hupp, J. T., *J. Phys. Chem.* **1990,** *94* (6), 2378-2380.

95. Weatherly, S. C.; Yang, I. V.; Thorp, H. H., *J. Am. Chem. Soc.* **2001,** *123* (6), 1236-1237.

96. Kundu, S.; Miceli, E.; Farquhar, E. R.; Ray, K., *Dalton Trans.* **2014,** *43*, 4264-4267.

97. Guttenplan, J. B.; Cohen, S. G., *J. Am. Chem. Soc.* **1972,** *94* (11), 4040-4042.

98. Wagner, P. J.; Lam, H. M. H., *J. Am. Chem. Soc.* **1980,** *102* (12), 4167-4172.

99. Lee, J. Y.; Peterson, R. L.; Ohkubo, K.; Garcia-Bosch, I.; Himes, R. a.; Woertink, J.; Moore, C. D.; Solomon, E. I.; Fukuzumi, S.; Karlin, K. D., *J. Am. Chem. Soc.* **2014,** *136*, 9925-9937.

100. Garcia-Bosch, I.; Cowley, R. E.; Díaz, D. E.; Peterson, R. L.; Solomon, E. I.; Karlin, K. D., *J. Am. Chem. Soc.* **2017,** *139* (8), 3186-3195.

101. Luo, Y.-R., *Handbook of bond dissociation energies in organic compounds*. CRC press: 2002.

102. Warren, J. J.; Tronic, T. A.; Mayer, J. M., *Chem Rev* **2010,** *110* (12), 6961-7001.

103. Berkowitz, J.; Ellison, G. B.; Gutman, D., *J. Phys. Chem.* **1994,** *98*, 2744-2765.

TOC graphic:

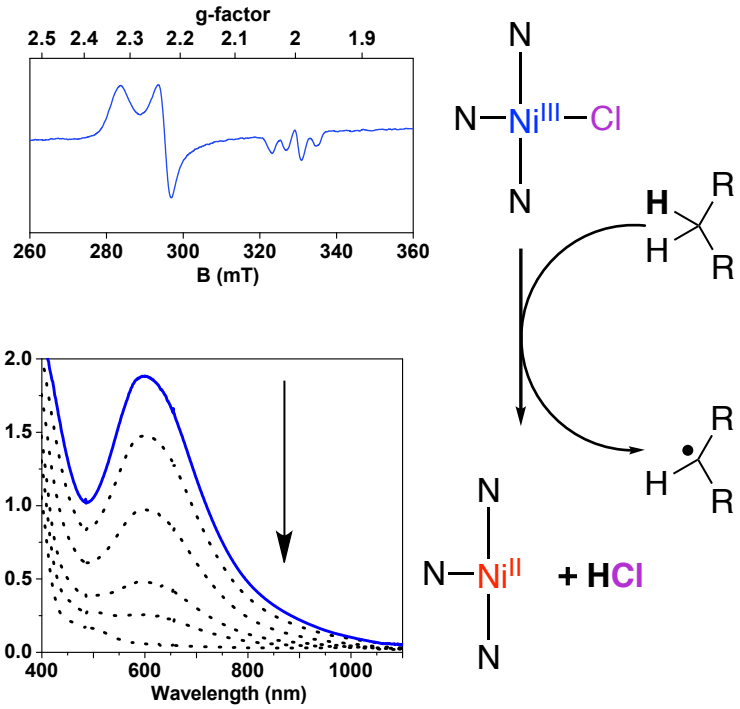
g-factor
2.5 2.4 2.3 2.2 2.1 2 1.9
260 280 300 320 340 360
B (mT)
2.0
1.5
1.0
0.5
0.0
400 600 800 1000
Wavelength (nm)
N
N—Ni^III—Cl
N
H
H
R
R
R
H
R
N
N—Ni^II
N
+ HCl